Acta Geophysica (2019) 67:1091–1106
https://doi.org/10.1007/s11600-019-00301-6

RESEARCH ARTICLE - APPLIED GEOPHYSICS

Random noise attenuation using a structure-oriented adaptive singular value decomposition

Yankai Xu[1] · Siyuan Cao[2] · Xiao Pan[3,4] · Wei Liu[2] · Hongling Chen[2]

Received: 24 October 2018 / Accepted: 8 May 2019 / Published online: 23 May 2019

Abstract
Singular value decomposition (SVD) is an efficient method to suppress random noise in seismic data. The performance of noise attenuation is typically affected by choosing the rank of the estimated signal using SVD. That the rank is fixed limits noise attenuation especially for a low signal-to-noise ratio data. Therefore, we propose a modified approach to attenuate random noise based on structure-oriented adaptively choosing singular values. In this approach, we first estimate dominant local slopes, predict other traces from a reference trace using the plane-wave prediction and construct a 3D seismic volume which is composed of all predicted traces. Then, we remove noise from a 2D profile whose traces are predicted from different reference traces via adaptive SVD filter (ASVD), which adaptively chooses the rank of estimated signal by the singular value increments. Finally, we stack every 2D denoised profile to a stacking denoised trace and reconstruct the 2D denoised seismic data which are composed of all stacking denoised traces. Synthetic data and field data examples demonstrate that the proposed structure-oriented ASVD approach performs well in random noise suppression for the low SNR seismic data with dipping and hyperbolic events.

Keywords Adaptive singular value decomposition · Singular value increments · Random noise attenuation · Plane-wave prediction

Introduction

Random noise has always been one of the important factors affecting the quality of seismic data. One of the main tasks of seismic data processing is to attenuate it. Many scholars have put forward and developed numerous effective approaches for random noise attenuation such as predict filter (Canales 1984; Liu and Liu 2011; Liu et al. 2012; Naghizadeh and Sacchi 2012), median filter (Liu et al. 2006; Zheng et al. 2017), empirical mode decomposition (EMD) (Cai et al. 2011; Chen et al. 2017; Liu et al. 2018), edge-preserving filtering (Yuan et al. 2018b) and some methods based on transform including the wavelet transform (Yang et al. 2017), the seislet transform (Fomel and Liu 2010) and sparsity dictionary (Beckouche and Ma 2014).

Singular value decomposition (SVD) filtering is a simple and powerful tool in random noise attenuation based on extracting the essential coherency components. Its performance of removing background noise is better than other denoising methods in seismic data with continuous unconflicting events (Bekara and Mirko 2007). Freire (1988) used it in the time-space (t-x) domain to separate noise with the upgoing and downgoing waves especially when the events are horizontal. Cadzow filtering (Trickett 2002; Trickett et al. 2003) can separate linear dipping coherent events from random noise because the rank of the Hankel matrix which is built from each frequency slice of linear events in the frequency-space (f-x) domain is equivalent to the number of their different slopes. Cadzow filtering is expanded to multiple dimensions (Oropeza and Sacchi 2011; Naghizadeh and Sacchi 2013,), called multichannel singular spectrum analysis (MSSA), via

✉ Siyuan Cao
csy@cup.edu.cn

Yankai Xu
xuyk163@163.com

1 College of Information Science and Engineering, China University of Petroleum-Beijing, Beijing, China

2 College of Geophysics, China University of Petroleum-Beijing, Beijing, China

3 Department of Earth and Space Sciences, Southern University of Science and Technology, Shenzhen, China

4 School of Earth and Space Science, University of Science and Technology of China, Hefei, China

embedding–deducting and restructuring the Hankel matrix in the f-x domain for 3D seismic volumes. Kreimer and Sacchi (2012) represented the spatial data at one frequency slice by a high-order tensor for denoising and interpolating of curved events. Huang et al. (2015) developed the MSSA algorithm by a damping factor controlling the degree of residual noise attenuation. However, the frequency-space (f-x) domain SVD methods, such as Cadzow filtering and MSSA, need to fit the assumption of a few linear events. To meet approximately linear and denoise effectively, Yuan and Wang (2011) presented that the seismic data in the t-x domain are preprocessed with a sliding window before using Cadzow filtering (called local Cadzow filtering). The denoising performance of the method is affected by the parameter of window length which is set more subjectively and experientially.

Local SVD (LSVD) (Bekara and Mirko 2007) is utilized by laterally aligning all coherent signal along dip direction within t-x domain local window. The method is not limited by the linear assumption. A structure-oriented SVD approach (SOSVD) (Gan et al. 2015) can enhance useful reflections via flattening predicted seismic events according to the estimated local dips. Although the structure-oriented-type approach requires prior flattening, which complicates the process, it has two advantages. First, both rank reduction of SVD and stacking can reduce noise. Second, without the limit of a uniform slope in processed windows, it is more effective in handling hyperbolic events and complex structures. However, the design that the rank of the estimated signal is fixed limits the denoised performance of SOSVD. If it can be adjusted according to the signal-to-noise ratio of the data, the effect of noise reduction will be improved.

In this paper, we propose a structure-oriented adaptive SVD (named SOASVD) approach for random noise attenuation. Firstly, we review the theory of SVD, analyze the distribution of singular values corresponding to random noise and put forward the concept of adjacent singular value increment and the method of adaptively choosing the rank of estimated signal. Then, we introduce the prediction of plane waves and combine it with ASVD for random noise attenuation of seismic data. Finally, we use the synthetic and field examples to compare the proposed algorithm with f-x deconvolution, f-x EMD, LSVD and local Cadzow filtering, and draw some conclusions.

Theory

SVD

Seismic data $\mathbf{D}$ consist of useful signal $\mathbf{S}$ and random noise $\mathbf{N}$, which is:

$$\mathbf{D} = \mathbf{S} + \mathbf{N} \tag{1}$$

where the size of matrixs $\mathbf{D}$, $\mathbf{S}$ and $\mathbf{N}$ is $N \times M$, M represents the number of seismic traces and N represents the number of time samples in the processed window. The SVD of matrix $\mathbf{D}$ can be expressed as (Vrabie et al. 2004):

$$\mathbf{D} = \mathbf{U}\sum\mathbf{V}^T = \sum_{\mathbf{k=1}}^{R} \sigma_k \mathbf{u}_k^T \tag{2}$$

where $\mathbf{U} = [\mathbf{u}_1, \mathbf{u}_2, ..., \mathbf{u}_k, ..., \mathbf{u}_R]$, $\mathbf{V} = [\mathbf{v}_1, \mathbf{v}_2, ..., \mathbf{v}_k, ..., \mathbf{v}_R]$, $\mathbf{u}_k$ and $\mathbf{v}_k$ are the eigenvectors, the matrix $\mathbf{u}_k\mathbf{v}_k^T$ is the eigenimages of $\mathbf{DD}^T$, $\sum = diag[\sigma_1, \sigma_2, ..., \sigma_k, ..., \sigma_R]$, $\sigma_1 \geq \sigma_2 \geq ...\sigma_k \geq ... \geq \sigma_R$, σ_k is the singular value and R is rank of $\mathbf{D}$. Equation (2) means that seismic data $\mathbf{D}$ include R eigenimages weighted by the corresponding singular values. Equation (2) can be also represented as (Freire 1988; Lu 2006) :

$$\mathbf{D} = \sum_{k=1}^{r} \sigma_k u_k v_k^T + \sum_{k=r+1}^{R} \sigma_k u_k v_k^T \tag{3}$$

where r is the rank of estimated seismic signal. Therefore, seismic data can be approximately divided into the seismic signal and random noise.

To effectively attenuate noise in seismic data using SVD method, we need to solve two problems. Firstly, we should obtain the events as horizontal as possible in processed windows. Secondly, the rank r needs to vary with the SNR of the seismic section. It is often set as 1 or 2 (Bekara and Mirko 2007), but it is only suitable for a single horizontal event with the fixed SNR. Lu (2006) suggests that it is given via the ratio of the stacking energy to the energy of the whole data. Freire (1988) refers that an abrupt change in the signal eigenvalues magnitude is easily distinguished from more gradual change in those of noise. However, the assumption is not proved and how to choose r based on the assumption is not given.

Singular value distribution of random noise

Assuming that the mean of random noise $\mathbf{N}$ is zero and its variance is σ^2, normally, it is considered that all singular values σ_{ni} for $\mathbf{N}$ are equal to $\sqrt{N}\sigma$. However, the singular value of noise σ_{ni} is also calculated by the equation:

$$\mathbf{nn}^T \simeq \begin{bmatrix} \sum_{j=1}^{N} n_{1,j}^2 & 0 & \cdots & \cdots & 0 \\ 0 & \ddots & 0 & \cdots & 0 \\ \vdots & 0 & \sum_{j=1}^{N} n_{i,j}^2 & 0 & \vdots \\ 0 & \cdots & 0 & \ddots & 0 \\ 0 & \cdots & \cdots & 0 & \sum_{j=1}^{N} n_{M,j}^2 \end{bmatrix} \tag{4}$$

where $\sigma_{n1}^2, \cdots, \sigma_{ni}^2, \ldots, \sigma_{nM}^2$ is the descending order of the collection $\left\{ \sum_{j=1}^{N} n_{1,j}^2, \ldots, \sum_{j=1}^{N} n_{i,j}^2, \ldots, \sum_{j=1}^{N} n_{M,j}^2 \right\}$ Defining a statistic variable $X = \sum_{j=1}^{N} n_{i,j}^2/\sigma^2$, X yields χ^2 distribution with the degree of freedom of N. When N is relatively large, then X approximately yields a normal distribution with the mean of N and variance of $2N$. Taking $Y = (X - N)/2N$, Y yields a standard normal distribution. If p denotes probability, u_p and u_a denote the quantile and upper quantile of Y. The relationship between u_p and u_a can be described as:

$$u_p = \begin{cases} -u_a & 0 < p < 0.5,\ p = a \\ 0 & p = 0.5 \\ u_a & 0.5 < p < 1,\ p = 1 - a \end{cases} \tag{5}$$

According to Yamauchi approximation, we have

$$u_a \approx \sqrt{z(2.0611786 - 5.7262204/(z + 11.640595)} \tag{6}$$

where $z = -ln(4a(1 - a))$. Therefore, the relationship between u_{xp} and p can be written as:

$$u_{xp} = \sqrt{2N}u_p + N \tag{7}$$

where u_{xp} represents the quantile of X and the relationship between u_{np} and p can be written as:

$$u_{np} = \sigma\sqrt{\sqrt{2N}u_p + N} \tag{8}$$

where u_{np} represents the quantile of σ_{ni}. Equations (5), (6) and (8) describe the relationship between u_{np} and p. It is equivalent to the relationship between σ_{ni} and the index i. We plot the curve of u_{np} with p ($N = 100$ and $\sigma = 0.1778$) in Fig. 1. It indicates that: 1) All singular values σ_{ni} are larger than zero and the mean value is about $\sqrt{N}\sigma$. 2) u_{np} is approximately linear with p from 0.1 to 0.9; in other words, the slope of u_{np} can be regarded as a constant. Therefore, the difference of adjacent singular values of **N** can be considered as a constant. 3) Both the slope of u_{np} and the mean of σ_{ni} increase with σ and N. So we define the difference between two adjacent singular values as the singular value increment:

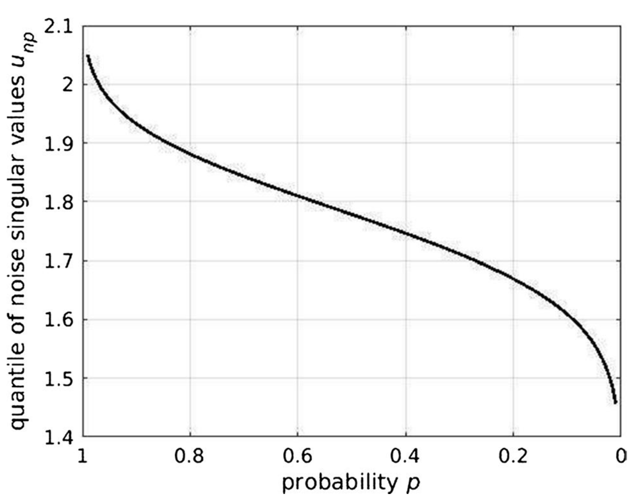

Fig. 1 The relationship between u_{np} and p

$$\Delta\sigma_i = \sigma_i - \sigma_{i+1} \tag{9}$$

Then, we have the following equation:

$$\Delta\overline{\sigma}_{ni} \approx (\sigma_{n1} - \sigma_{nN})/(N - 1) < \sigma_{n1}/(N - 1) \tag{10}$$

where $\Delta\overline{\sigma}_{ni}$, σ_{n1} and σ_{nN} are the mean of adjacent singular value increments, the maximum singular value and the minimum singular value corresponding to random noise, respectively.

Adaptive SVD

Different from random noise, seismic signal may be reconstructed from only a few of the first eigenimages because of their high correlation. The high correlation has been commonly utilized to seismic data processing (Yuan et al. 2018a; Ma et al. 2018; Shi et al. 2018). Increments of adjacent singular values corresponding to seismic signal can be characterized by the following equation:

$$\Delta\sigma_{sm} > \sigma_{s1}/(N - 1) \tag{11}$$

where $\triangle\sigma_{sm}$ and σ_{s1} are the maximum adjacent singular value increment and the maximum singular value corresponding to seismic signal, respectively. Comparing Eqs. (10) and (11), it is derived:

$$\Delta\sigma_{sm}/\Delta\overline{\sigma}_{ni} > \sigma_{s1}/\sigma_{n1} \tag{12}$$

Equation (12) indicates that the seismic events can be better separated from noise by choosing the rank r by the singular value increments than the singular values. The r is varied with the singular value increments corresponding to seismic signal and noise using ASVD algorithm. The main flowchart of ASVD is as follows:

1. Determine a threshold by the mean of singular value increments corresponding to noise;
2. Determine the rank r through comparing the first few singular value increments with the threshold.

Prediction of plane waves

The input matrix of ASVD algorithm should be adjusted as horizontal as possible, so we apply the prediction of plane waves to it. The local plane differential equation is expressed as:

$$\frac{\partial D}{\partial x} + \alpha\frac{\partial D}{\partial t} = 0 \tag{13}$$

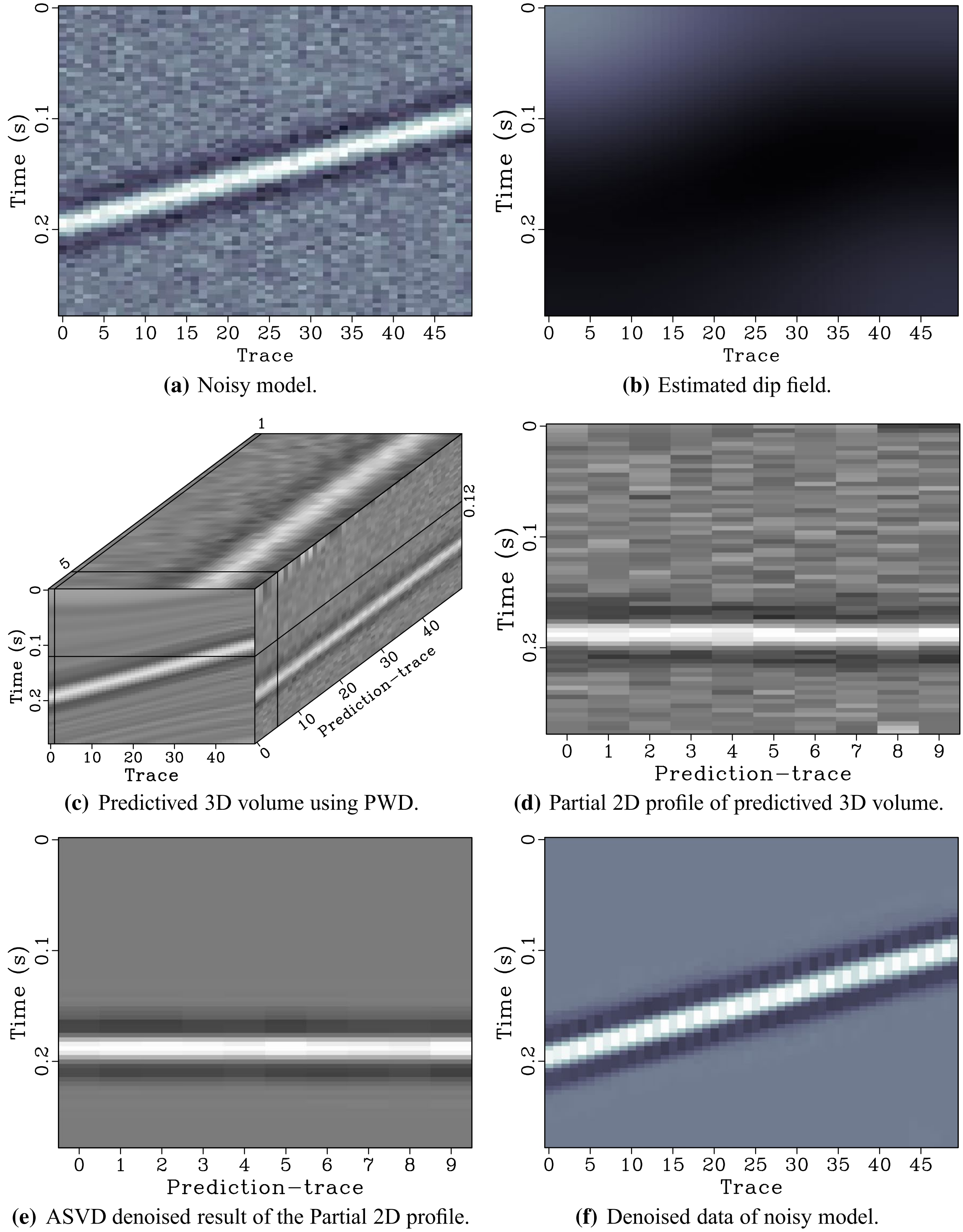

(a) Noisy model. **(b)** Estimated dip field. **(c)** Predictived 3D volume using PWD. **(d)** Partial 2D profile of predictived 3D volume. **(e)** ASVD denoised result of the Partial 2D profile. **(f)** Denoised data of noisy model.

Fig. 2 Demonstration for SOASVD method

where α is the local seismic dip. The solution of Eq. (13) can be given as (Fomel 2002; Liu et al. 2015):

$$\mathbf{d}_{(x+1)} = \mathbf{d}_{(x)}\mathbf{p}_{(x\rightarrow x+1)} \tag{14}$$

where $\mathbf{d}_{(x)}$ is the data of trace x. $\mathbf{p}_{(x\rightarrow x+1)}$ represents a prediction matrix from trace x to trace $x+1$ and is a function of $\boldsymbol{\alpha}$. The local seismic dip $\boldsymbol{\alpha}$ is optimized by solving the following least-squares minimization problem:

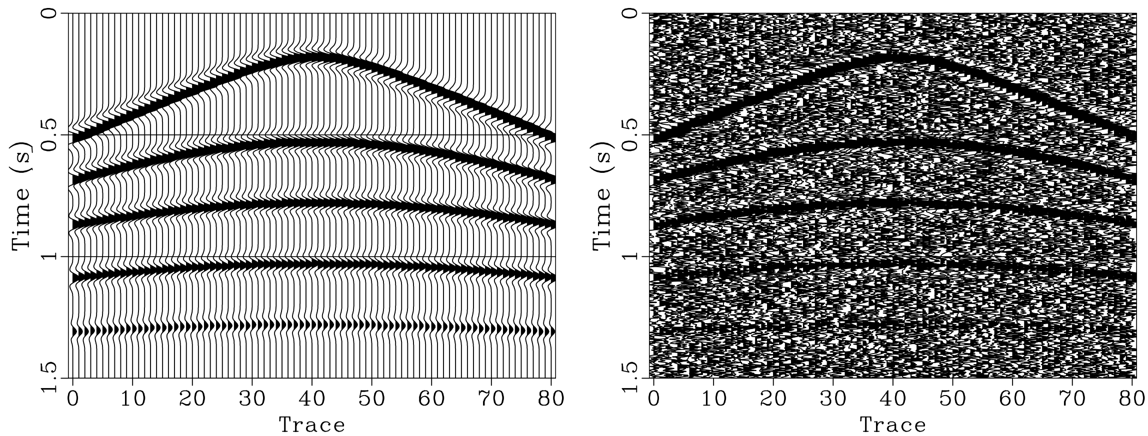

(a) Clean data.
(b) Noisy data.

Fig. 3 Hyperbolic-events synthetic seismic example

$$\tilde{\boldsymbol{\alpha}} = \arg min \|\mathbf{W}(\boldsymbol{\alpha})\mathbf{D}\|_2^2 \tag{15}$$

$$\text{where } \mathbf{W}(\boldsymbol{\alpha}) = \begin{bmatrix} \mathbf{I} & 0 & 0 & \cdots & 0 \\ -\mathbf{p}_{(1\to2)} & \mathbf{I} & 0 & \cdots & 0 \\ 0 & -\mathbf{p}_{(2\to3)} & \mathbf{I} & \cdots & 0 \\ \cdots & \cdots & \cdots & \cdots & \cdots \\ 0 & 0 & 0 & -\mathbf{p}_{(N-1\to N)} & \mathbf{I} \end{bmatrix},$$

$\mathbf{I}$ is the identity matrix. Let $\tilde{\mathbf{D}}_1$ represent a collection of predicted traces from the reference trace $\mathbf{d}_1$, $\tilde{\mathbf{D}}_1$ can be calculated (Fomel 2002):

$$\tilde{\mathbf{D}}_1^T = \mathbf{P}_{(1\to i)}^T \mathbf{d}_1 \tag{16}$$

where $\tilde{\mathbf{D}}_1 = [\tilde{\mathbf{d}}_{(1\to1)}, \tilde{\mathbf{d}}_{(1\to2)}, \tilde{\mathbf{d}}_{(1\to3)}, \cdots, \tilde{\mathbf{d}}_{(1\to N)}]$ and $\mathbf{P}_{(1\to i)} = [\mathbf{I}, \mathbf{p}_{(1\to2)}, \mathbf{p}_{(1\to3)}, \cdots, \mathbf{p}_{(1\to N)}]$. Then, we can predict $\tilde{\mathbf{D}}_i$ from a reference trace i $(i = 1, 2, \cdots, N)$. Therefore, a 3D predicted volume from a 2D seismic data is created. A 2D profile of the 3D predicted volume is composed of predicted traces $\tilde{\mathbf{d}}_{(1\to x)}, \tilde{\mathbf{d}}_{(2\to x)}, \tilde{\mathbf{d}}_{(3\to x)}, \cdots, \tilde{\mathbf{d}}_{(N\to x)}$, which have high similarity with the primitive trace x.

SOASVD denoising

The ASVD is applied to the 2D profile with approximate flat events. It is a structure-oriented ASVD (SOASVD) denoising approach. The detailed steps are shown below:

1. Estimate dominant local slopes.
2. Predict other traces from a reference trace i $(i = 1, \ldots, N)$ by applying plane-wave destruction filter which are designed by using the estimated slope. A 3D seismic volume is composed of all predict traces.
3. Apply ASVD filter to a 2D profile of the 3D seismic volume for denoising.
4. Stack the output of step 3).
5. Repeat steps 3) and 4) until all 2D profiles are processed and stacked.

Figure 2 demonstrates the process of SOASVD. Figure 2a is the original noisy model. Figure 2b is the estimated dip field of noisy model. A front view of Fig. 2c is the predicted traces from a reference trace applying the plane-wave destruction filter, and a profile view of Fig. 2c is the prediction of a primitive trace from all reference traces. Figure 2d is the partial profile view which is close to the primitive trace. Figure 2e is the denoised result of Fig. 2d using ASVD method. Figure 2f is the final denoised result of Fig. 2a, and every trace in the figure is formed by the stacked trace of a denoised 2D profile.

Examples

Synthetic examples

To test the performance of the proposed algorithm, we use two synthetic examples in this section. The first example is a simple seismic profile including five hyperbolic events. The data consist of 81 traces with a sampling rate of 4 ms. The total time is 1.5 s. The slopes of five events become gradually smaller from the top to the bottom. The amplitudes of five events are 3, 2.5, 2, 1.5 and 0.8 from the top to the bottom, respectively. The clean data and noisy data with SNR of −4.074 dB are shown in Fig. 3. For f-x deconvolution, f-x EMD and local Cadzow filtering, the range of frequency is set from 2 Hz to 75 Hz. For local Cadzow filtering, LSVD and LASVD, we use the sliding window consisting of 20 traces and 50 time samples. For local Cadzow filtering and

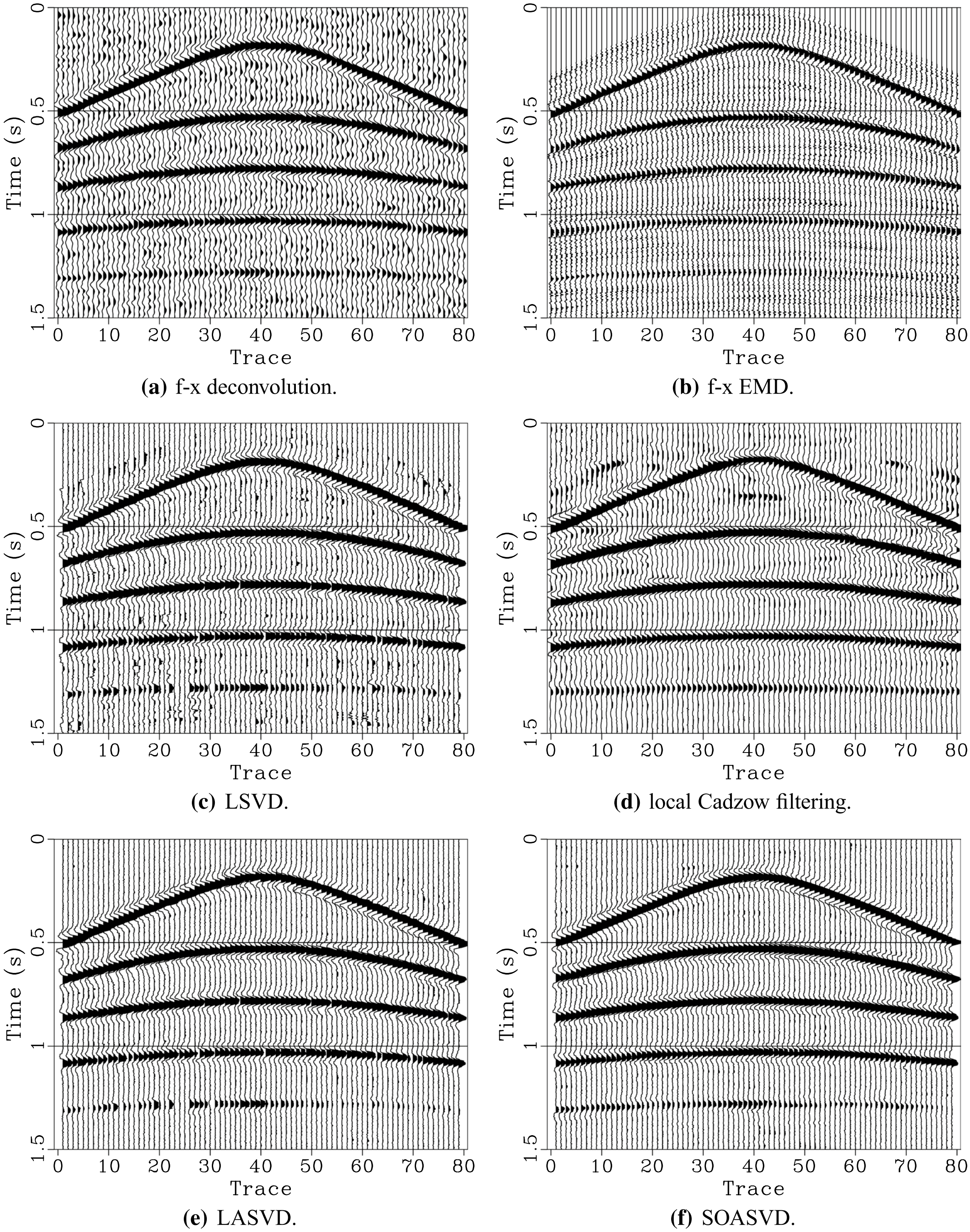

(a) f-x deconvolution.
(b) f-x EMD.
(c) LSVD.
(d) local Cadzow filtering.
(e) LASVD.
(f) SOASVD.

Fig. 4 Comparison of denoised data for the hyperbolic-events synthetic example

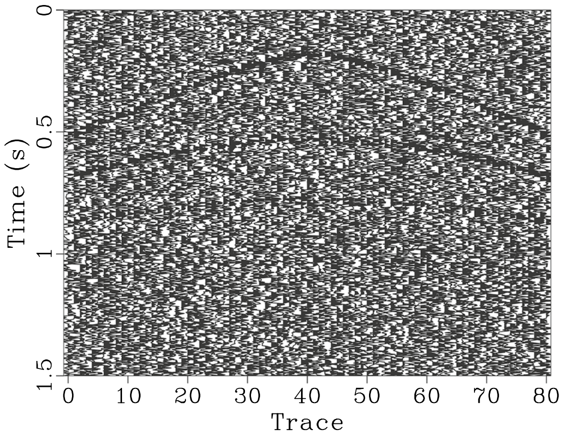

(a) f-x deconvolution.

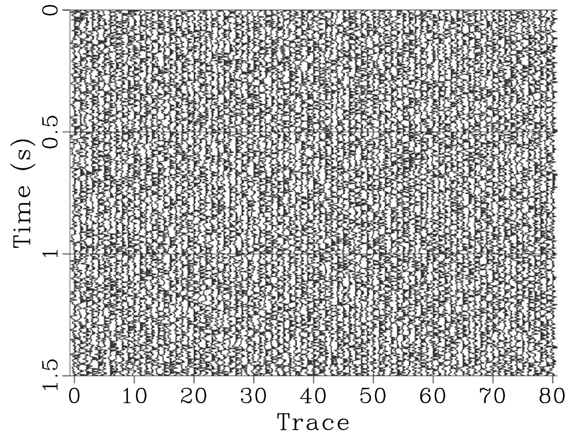

(b) f-x EMD.

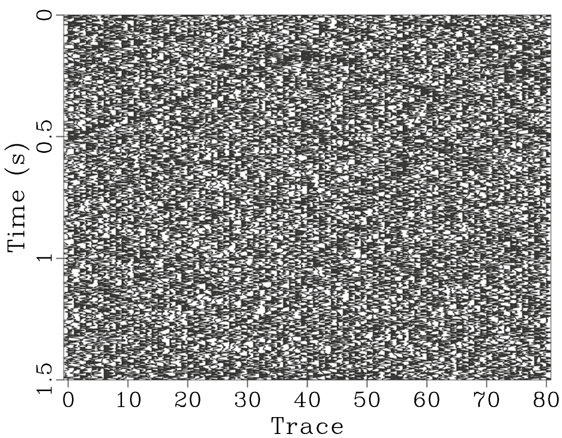

(c) LSVD.

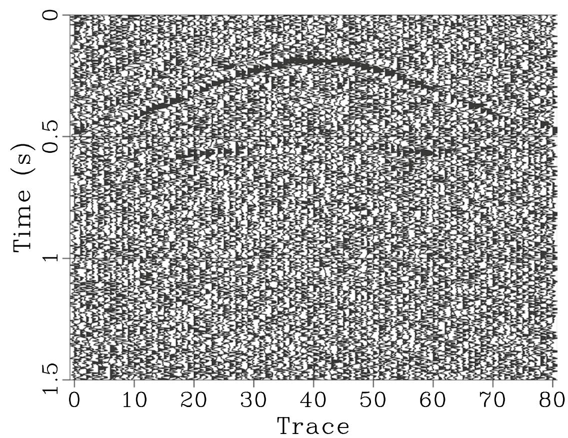

(d) local Cadzow filtering.

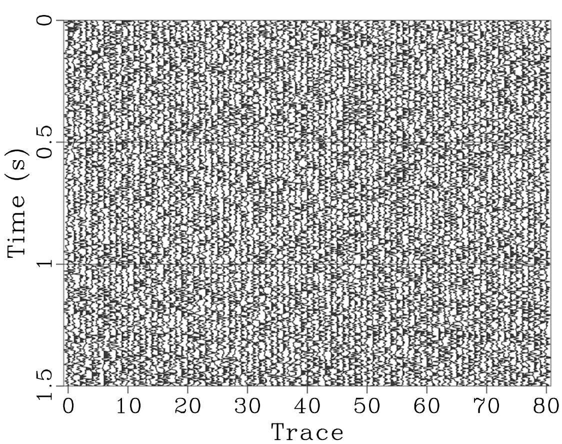

(e) LASVD.

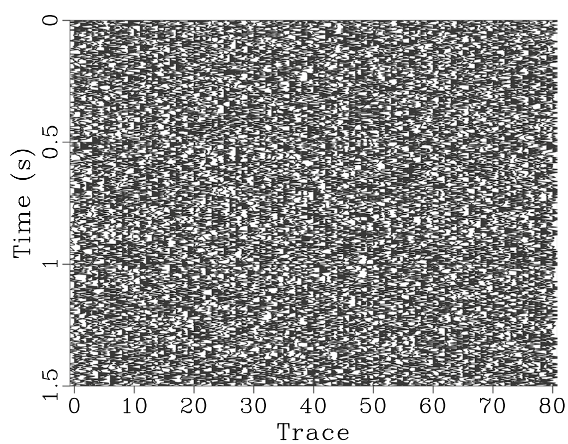

(f) SOASVD.

Fig. 5 Comparison of removed noise for the hyperbolic-events synthetic example

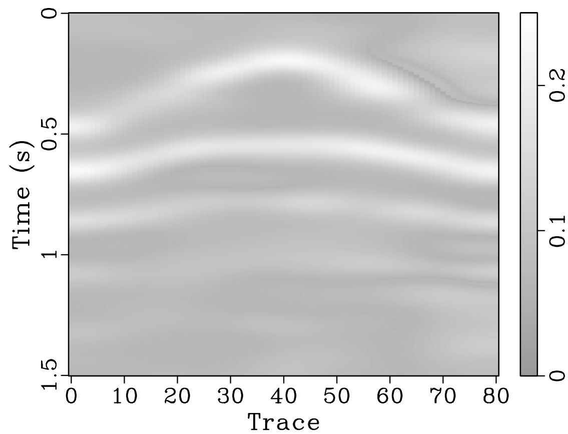

(a) f-x deconvolution.

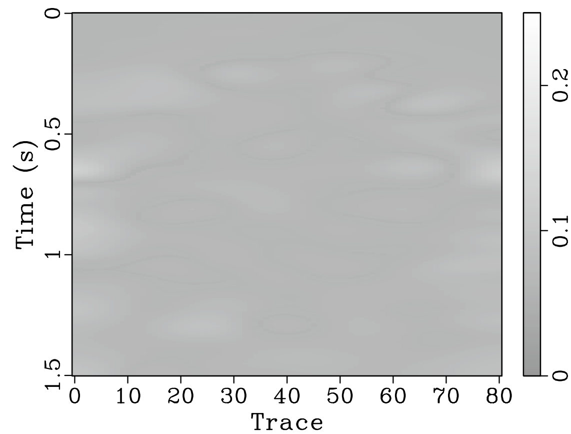

(b) f-x EMD.

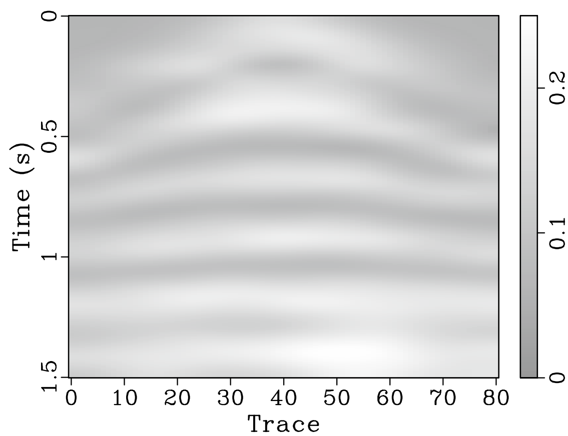

(c) LSVD.

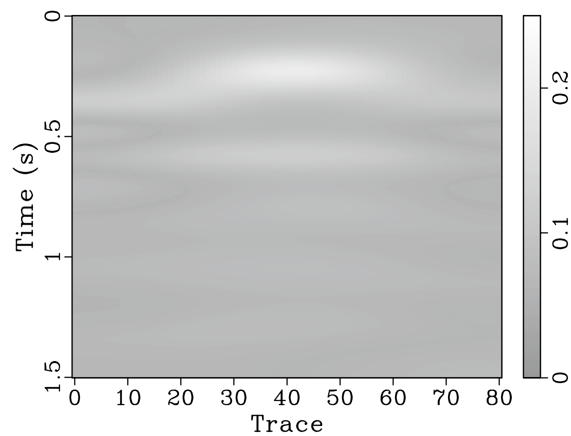

(d) local Cadzow filtering.

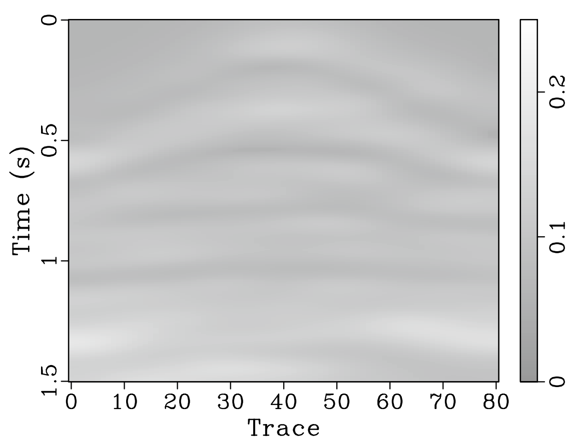

(e) LASVD.

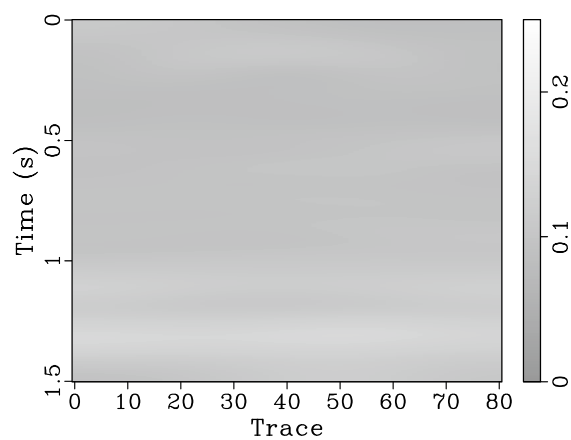

(f) SOASVD.

Fig. 6 Cross-correlation of denoised data and, respectively, removed noise for the hyperbolic-events synthetic example

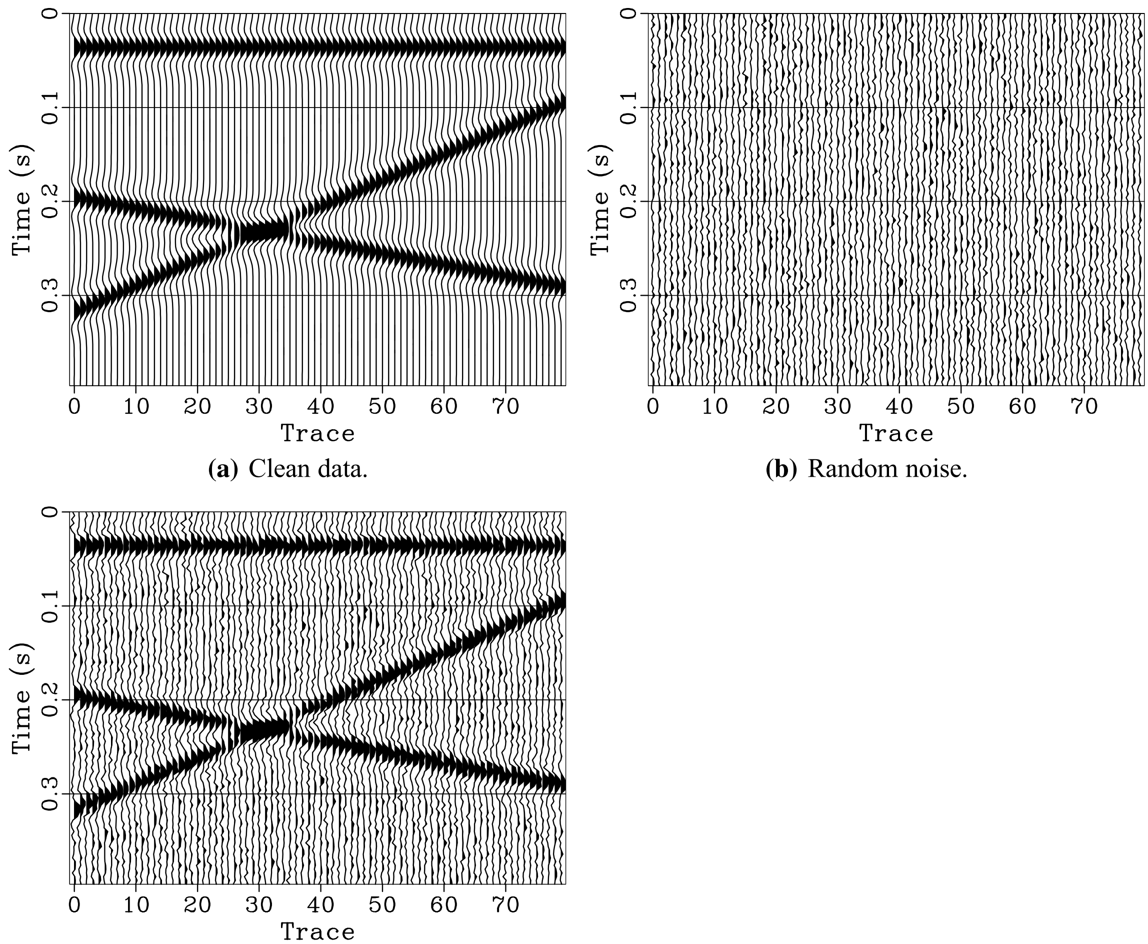

(a) Clean data. **(b)** Random noise. **(c)** Noisy data.

Fig. 7 Conflicted linear synthetic seismic profile

LSVD, we set the rank r to be 2. For LASVD and SOASVD, we set the threshold as $4 \triangle \overline{\sigma}_{ni}$. The denoised results using f-x deconvolution, f-x EMD, LSVD, local Cadzow filtering, LASVD and SOASVD algorithm are shown in Fig. 4. We can see that the denoised result using f-x deconvolution (Fig. 4a) has obvious residual noise. Compared with local Cadzow filtering, LSVD, f-x EMD and f-x deconvolution, LASVD and SOASVD are more effective in removing noise. The removed noise sections are displayed in Fig. 5. We can also observe five hyperbolic leakage events from the removed noise section using f-x deconvolution in Fig. 5a and some visible leakage energy to the high slope event for LSVD (Fig. 5c) and local Cadzow filtering (Fig. 5d). There are little visible events using f-x EMD (Fig. 5b), LASVD (Fig. 5e) and SOASVD approach (Fig. 5f). To measure the leakage energy, we evaluate the cross-correlation sections between the denoised data and the corresponding removed noise shown in Fig. 6. The cross-correlation section in Fig. 6f illustrates that the leakage energy using SOASVD approach is least. For numerically comparing the denoising performances of these approaches, we evaluate the SNR of results processed with five approaches and list them in Table 1. The SNR of input noisy data in experiment one is −4.074 dB. The SNR using f-x deconvolution, f-x EMD, LSVD, local Cadzow filtering, LASVD and SOASVD approaches is 5.780 dB, 6.634 dB, 6.542 dB,7.237 dB, 9.709 dB and 12.047dB, respectively. The SNR of input noisy data in experiment two is −6.974 dB, and the SNR after processing using these approaches is 4.785 dB, 4.75 dB, 4.897 dB, 5.785 dB, 7.741 dB and 9.238 dB, respectively. SOASVD approach yields the best result for noise attenuation.

The second synthetic example contains conflicting linear events. The clean data (Fig. 7a) include one horizontal event and two dipping events. The noisy data are shown in Fig. 7c after adding random noise (Fig. 7b). Figures 8, 9 and 10 show the denoised results, the removed noise sections and their corresponding cross-correlation sections. The denoised results (Fig. 8a–d) by using f-x deconvolution, f-x EMD, LSVD and local Cadzow filtering are still contaminated by a certain amount of noise. Compared

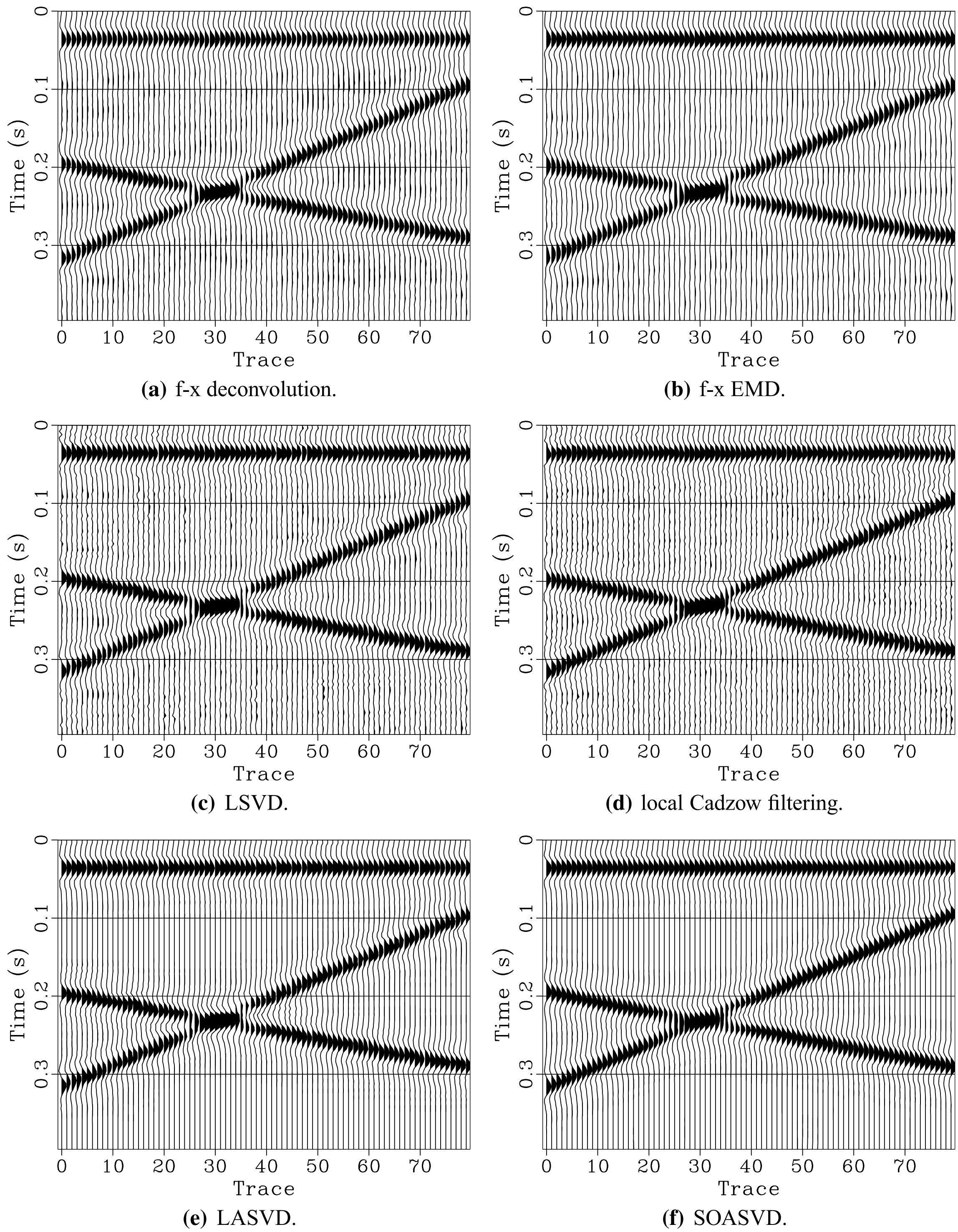

Fig. 8 Comparison of denoised data for the conflicted linear synthetic example

with them, Fig. 8e, f shows that random noise is largely suppressed. The removed noise (Fig. 9a–c) still has visible coherent events. From Figures 8f, 9f and 10f, it can be observed that SOASVD has the best performance in removing noise and preserving the useful signal except leaking a little energy in conflicted point of events. The processed result using the local orthogonalization method (Fomel 2007; Chen and Fomel 2015) is shown in Fig. 11.

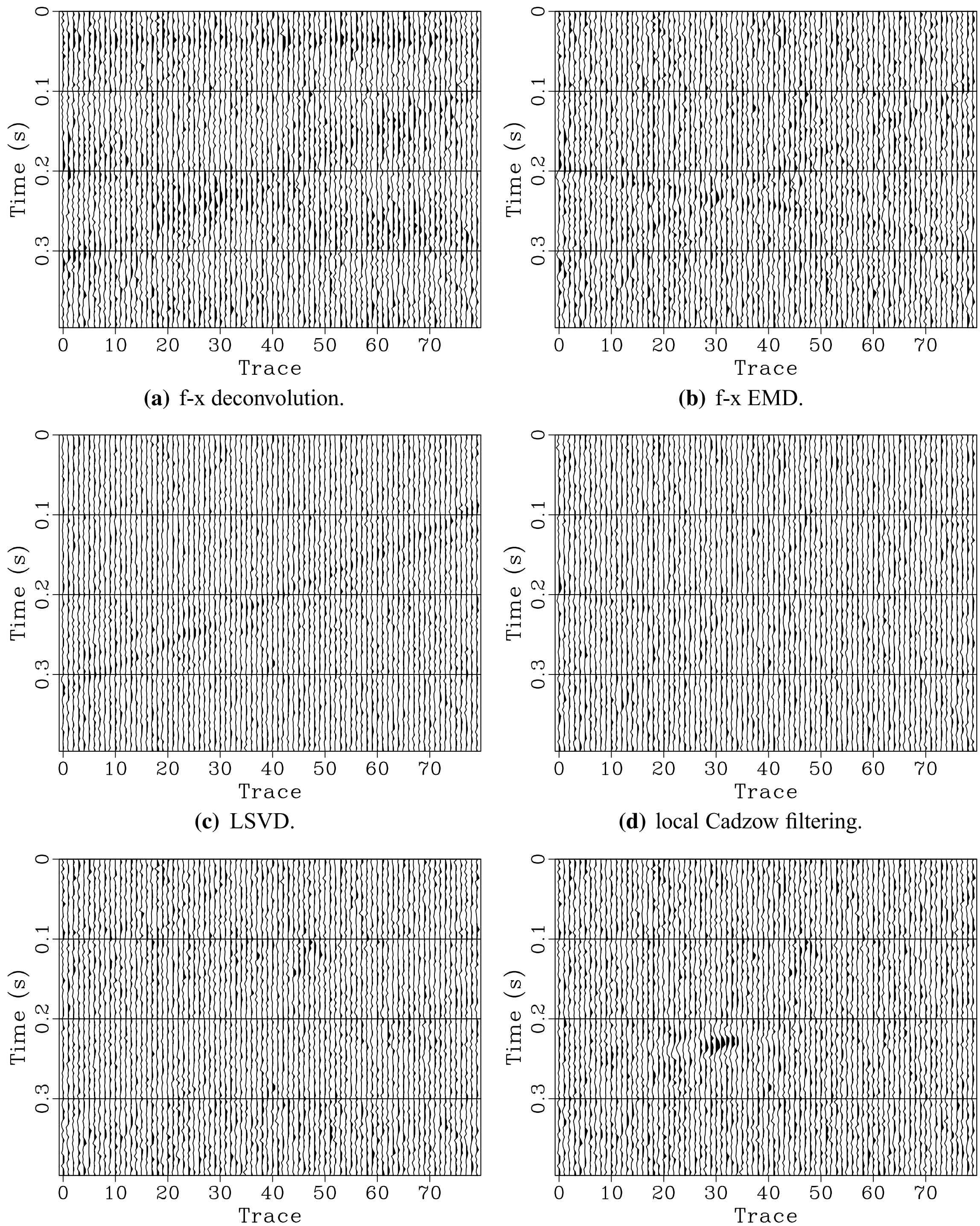

(a) f-x deconvolution. **(b)** f-x EMD. **(c)** LSVD. **(d)** local Cadzow filtering. **(e)** LASVD. **(f)** SOASVD.

Fig. 9 Comparison of removed noise for the conflicted linear synthetic example

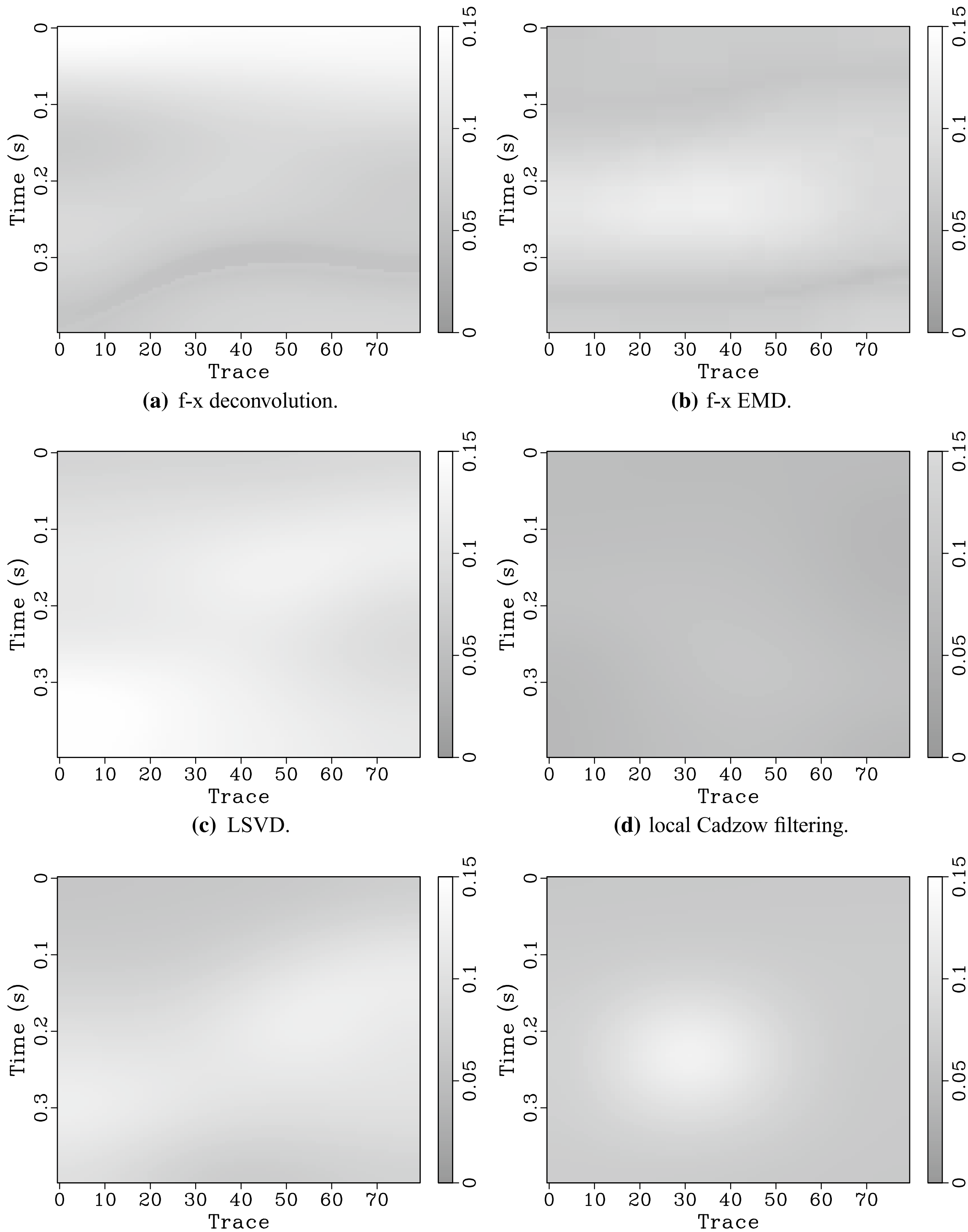

(a) f-x deconvolution.

(b) f-x EMD.

(c) LSVD.

(d) local Cadzow filtering.

(e) LASVD.

(f) SOASVD.

Fig. 10 Cross-correlation of denoised data and, respectively, removed noise for the conflicted linear synthetic example.

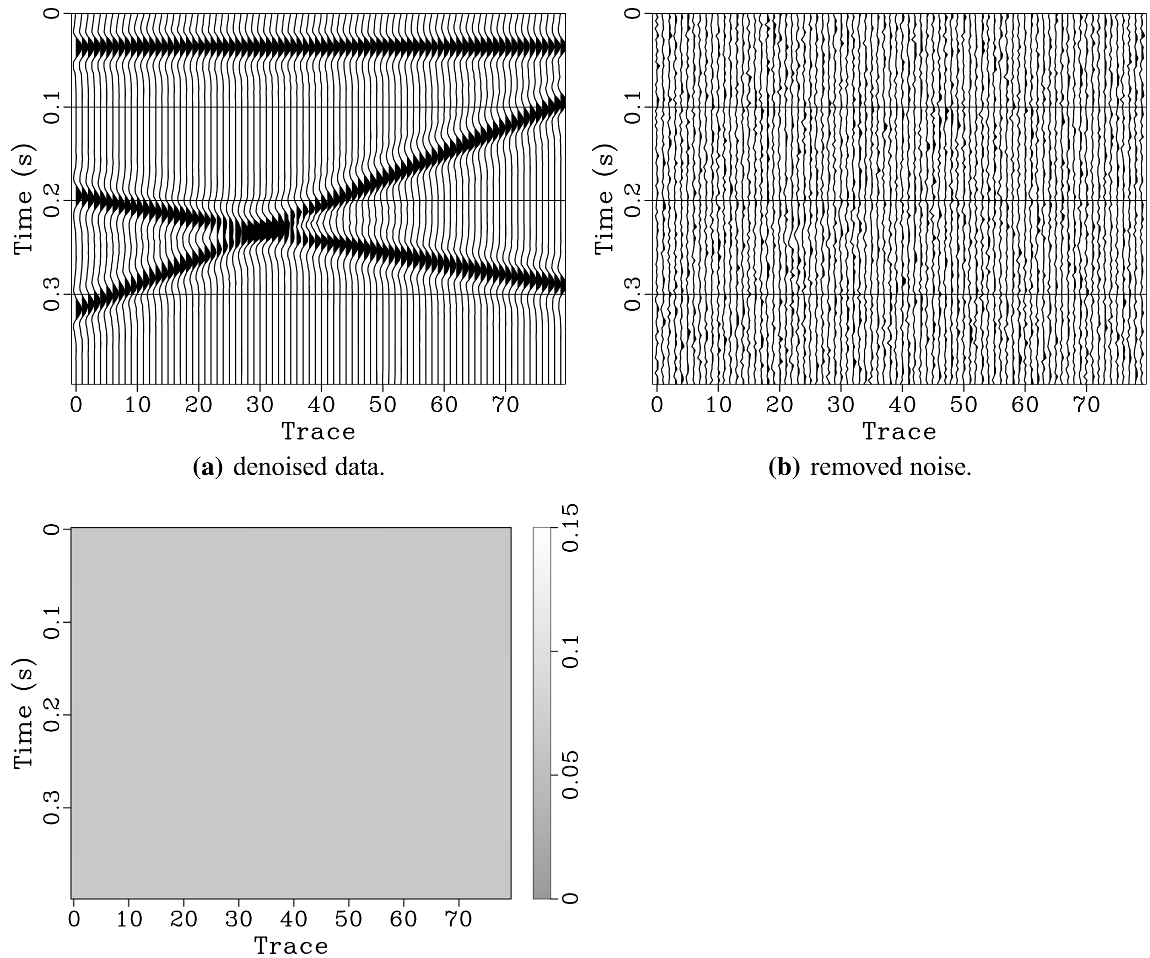

(a) denoised data. **(b)** removed noise. **(c)** cross-correlation.

Fig. 11 SOASVD orthogonalization for the conflicted linear synthetic example

Comparing Fig. 11b, c with Figs. 9f, 10f illustrates that the leaked useful signal in conflicted point is effectively retrieved.

Field data example

To further demonstrate the performance of SOASVD in practice, we choose the 2D profile (Fig. 12a) from western China. There are 57 traces with a sampling rate of 1 ms. It can be observed that strong random noise is present in data. After applying f-x deconvolution, f-x EMD, LSVD, local Cadzow filtering and SOASVD methods, the denoised result and the removed noise are shown in Figs. 12 and 13, respectively. Random noise around at about 0.2 s is effectively attenuated by using f-x deconvolution, f-x EMD, LSVD and local Cadzow filtering approaches, while their performance is poor at about 0.3 s–0.5 s. Figures 12f and 13e show the information of events is well preserved and noise is suppressed using SOASVD method. It is noted that the dominant local slopes are estimated from Fig. 12b.

Limitations and future work

The SOASVD approach has its own limitations. The main limitation is that seismic events are attenuated or distorted at the crossed points because the predicted traces have lower similarity with the primitive trace in the region of the crossed points. Although the performance has improved by using the local orthogonalization, the investigation of noise attenuation regarding crossed points may be the subject of our future work.

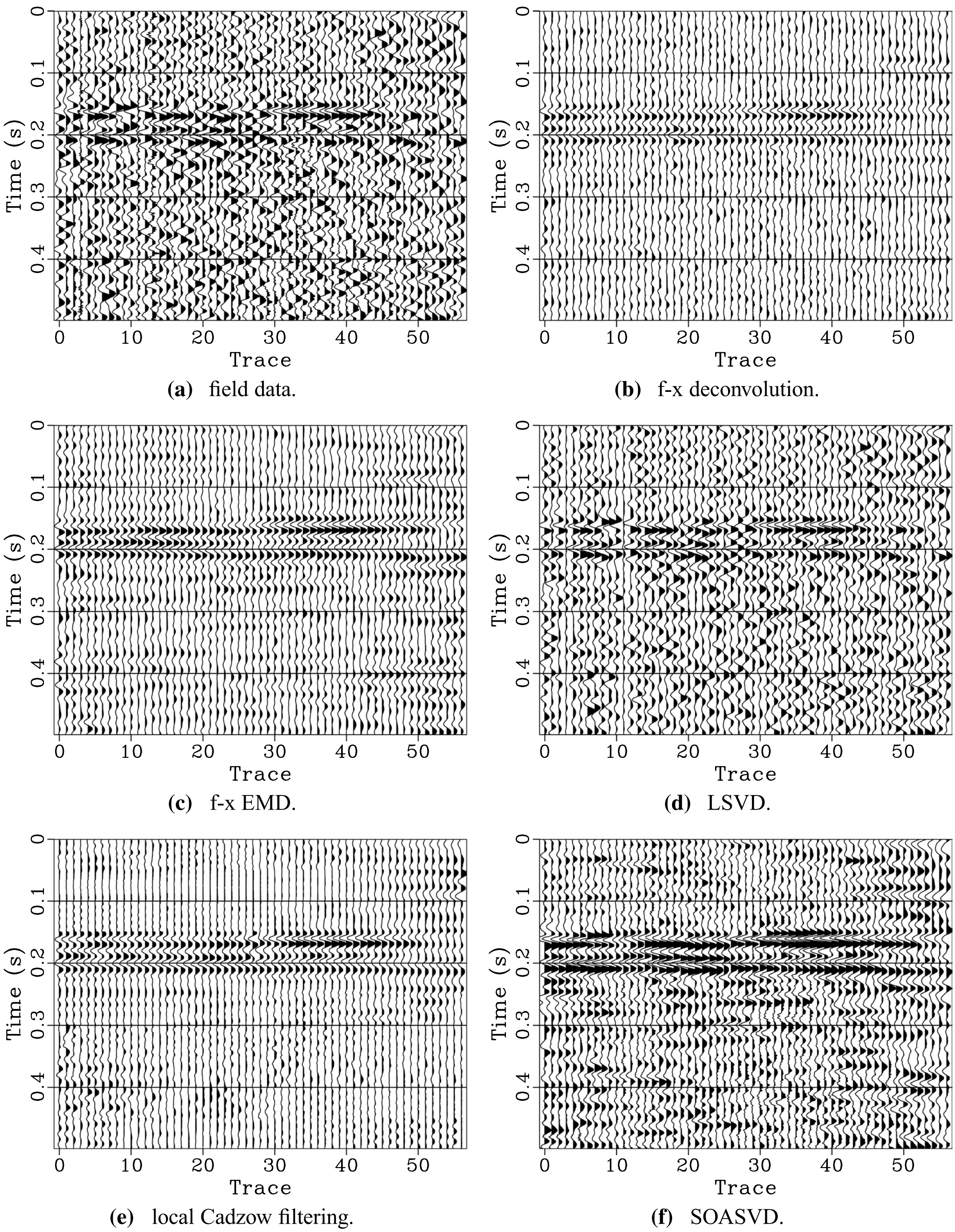

Fig. 12 Comparison of denoised results for field data

Conclusions

We put forward a approach to attenuate random noise using structure-oriented adaptive singular value decomposition (SOASVD). With the approach, each trace is extended to a flat 2D profile via predicting the trace from its neighboring traces. After noise is attenuated, the predicted 2D profile is stacked as one trace. Random noise of the predicted flat 2D profile is attenuated by using ASVD filter which can adaptively choose the rank of the estimated signal according

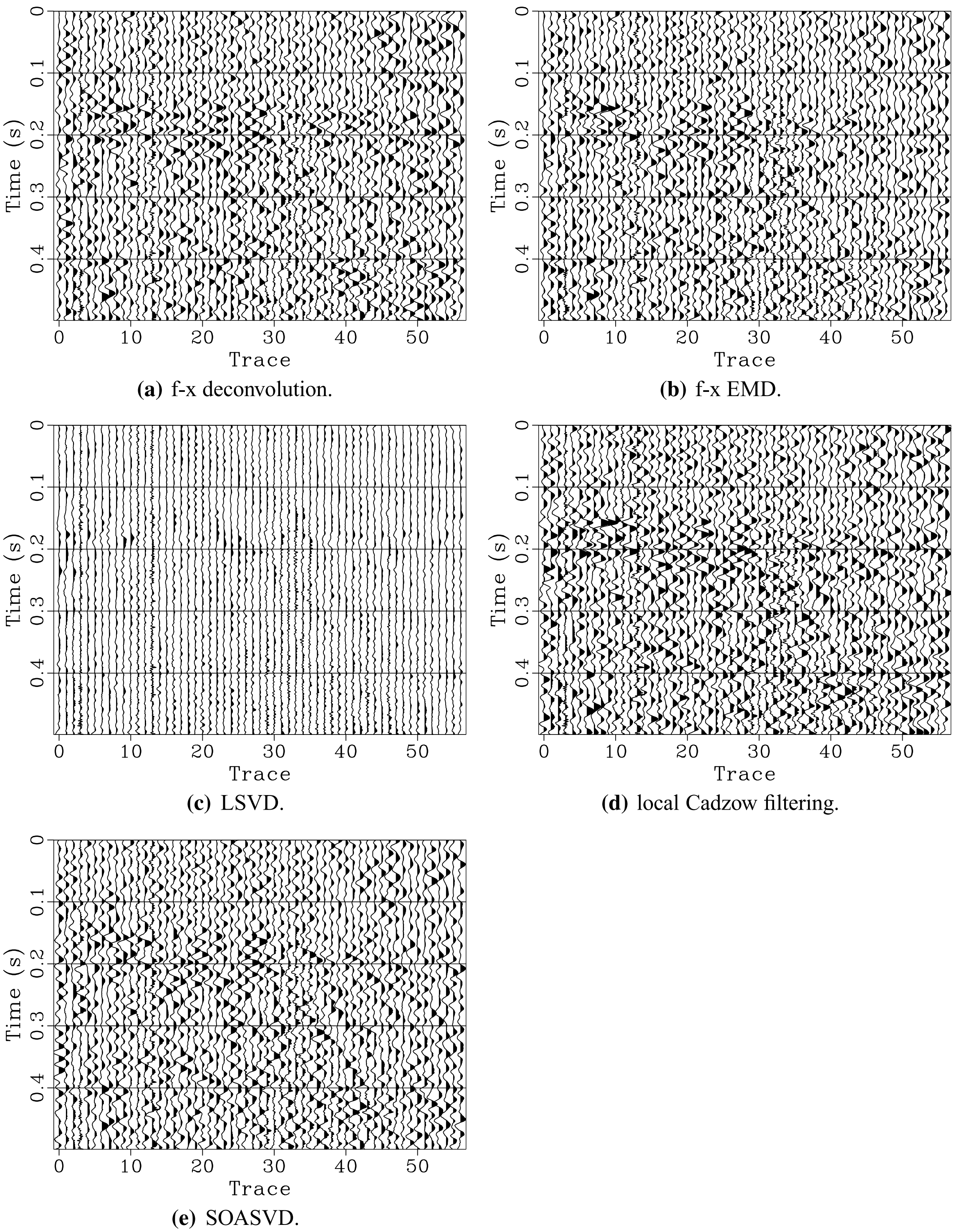

(a) f-x deconvolution.

(b) f-x EMD.

(c) LSVD.

(d) local Cadzow filtering.

(e) SOASVD.

Fig. 13 Comparison of denoised results for field data

Table 1 Comparison of SNR using different approaches

Test	Original	f-x filter	f-x EMD	LSVD	Local Cadzow	LASVD	SOASVD
Exp one(dB)	−4.074	5.780	6.634	6.542	7.237	9.709	12.047
Exp two(dB)	−6.974	4.785	4.750	4.897	5.785	7.741	9.238

to the adjacent singular value increment and the SNR of processed windows. Synthetic and field data examples demonstrate that, compared with f-x deconvolution, f-x EMD, LSVD and local Cadzow filtering, the proposed approach can obtain the best performance in suppressing random noise and preserving the useful signals for the low SNR data with dipping and hyperbolic events .

Acknowledgements We would like to thank Yufeng Wang for inspiring discussions and help with the code in the Madagascar software package. This work is financially supported by Petro China Innovation Foundation (2017D-5007-0302), National Natural Science Foundation of China (41674128) and the National Key Research and Development Program of China (SQ2017YFGX030021).

References

Beckouche S, Ma J (2014) Simultaneous dictionary learning and denoising for seismic data. Geophysics 79(3):A27–A31

Bekara M, Mirko VDB (2007) Local singular value decomposition for signal enhancement of seismic data. Geophysics 72(2):V59–V65

Cai HP, He ZH, Huang DJ (2011) Seismic data denoising based on mixed time frequency methods. Appl Geophys 8(4):319–327

Canales LL (1984) Random noise reduction. SEG Tech Progr Expand Abstr 3(1):329–329

Chen Y, Fomel S (2015) Random noise attenuation using local signal and noise orthogonalization. Geophysics 80(6):WD1–WD9

Chen Y, Zhou Y, Chen W, Zu S, Huang W, Zhang D (2017) Empirical low rank approximation for seismic noise attenuation. IEEE Trans Geosci Remote Sens 55(8):4696–4711

Fomel S (2007) Shaping regularization in geophysical estimation problems. Geophysics 72(2):R29–R36

Fomel S (2002) Applications of plane wave destruction filters. Geophysics 67(10):1946–1960

Fomel S, Liu Y (2010) Seislet transform and seislet frame. Geophysics 75(3):V25–V38

Freire SLM (1988) Application of singular value decomposition to vertical seismic profiling. Geophysics 53(6):778–785

Gan S, Chen Y, Zu S, Qu S, Zhong W (2015) Structure oriented singular value decomposition for random noise attenuation of seismic data. J Geophys Eng 12(2):262–272

Huang W, Wang R, Chen Y, Li H, Gan S (2015) Damped multichannel singular spectrum analysis for 3D random noise attenuation. Geophysics 81(4):V261–V270

Kreimer N, Sacchi MD (2012) A tensor higher order singular value decomposition for prestack seismic data noise reduction and interpolation. Geophysics 77(3):V113–V122

Liu C, Liu Y, Yang B, Wang D, Sun J (2006) A 2D multistage median filter to reduce random seismic noise. Geophysics 71(5):V105–V110

Liu C, Chen C, Wang D, Liu Y, Wang S, Zhang L (2015) Seismic dip estimation based on the two dimensional Hilbert transform and its application in random noise attenuation. Appl Geophys 12(1):55–63

Liu G, Chen X, Du J, Wu K (2012) Random noise attenuation using f-x regularized nonstationary autoregression. Geophysics 77(2):V61–V69

Liu W, Cao S, Jin Z, Wang Z, Chen Y (2018) A novel hydrocarbon detection approach via high-resolution frequency dependent avo inversion based on variational mode decomposition. IEEE Trans Geosci Remote Sens 56(4):2007–2024

Liu Y, Liu C (2011) Nonstationary signal and noise separation using adaptive prediction error filter. In: SEG technical program expanded, pp 3601–3606

Lu W (2006) Adaptive noise attenuation of seismic images based on singular value decomposition and texture direction detection. J Geophys Eng 3(3):28–34

Ma M, Wang S, Yuan S, Gao J, Li S (2018) Multichannel block sparse Bayesian learning reflectivity inversion with lp-norm criterion-based Q estimation. J Appl Geophys 159:434–445

Naghizadeh M, Sacchi M (2012) Multicomponent f-x seismic random noise attenuation via vector autoregressive operators. Geophysics 77(2):V91–V99

Naghizadeh M, Sacchi M (2013) Multidimensional de-aliased Cadzow reconstruction of seismic records. Geophysics 78(1):A1–A5

Oropeza V, Sacchi M (2011) Simultaneous seismic data denoising and reconstruction via multichannel singular spectrum analysis. Geophysics 76(3):V25–V32

Shi P, Yuan S, Wang T, Wang Y, Liu T (2018) Fracture identification in a tight sandstone reservoir: a seismic anisotropy and automatic multisensitive attribute fusion framework. IEEE Geosci Remote Sens Lett 15(10):1525–1529

Trickett SR (2002) Fx eigenimage noise suppression. SEG technical program expanded abstracts 72th Annual international meeting: 2166–2169

Trickett SR, Grimm J, Aleksic V, Mcvee DJ (2003) F-xy eigenimage noise suppression. Geophysics 68(2):751–759

Vrabie VD, Mars JI, Lacoume JL (2004) Modified singular value decomposition by means of independent component analysis. Signal Process 84(3):645–652

Yang H, Long Y, Lin J, Zhang F, Chen Z (2017) A seismic interpolation and denoising method with curvelet transform matching filter. Acta Geophys 65(5):1029–1042

Yuan S, Wang S (2011) A local f-x Cadzow method for noise reduction of seismic data obtained in complex formations. Pet Sci 8(3):269–277

Yuan S, Liu J, Wang S, Wang T, Shi P (2018a) Seismic waveform classification and first-break picking using convolution neural networks. IEEE Geosci Remote Sens Lett 15(2):272–276

Yuan S, Wang S, Luo C, Wang T (2018b) Inversion-based 3-D seismic denoising for exploring spatial edges and spatio-temporal signal redundancy. IEEE Geosci Remote Sens Lett 15(11):1682–1686

Zheng J, Lu J, Jiang T, Liang Z (2017) Microseismic event denoising via adaptive directional vector median filters. Acta Geophys 65(1):47–54